# High-velocity impact damage modeling of laminated composites using Abaqus/Explicit and multiscale methods

I. Smojver and D. Ivančević

Department of Aeronautical Engineering, Faculty of Mechanical Engineering and Naval Architecture, University of Zagreb

I. Lučića 5, HR-10000, Zagreb, Croatia

***Abstract***: *The present work describes a multiscale methodology which has been developed for modeling of impact damage in the laminated composite structures. The methodology employs the High Fidelity Generalized Method of Cells (HFGMC) micromechanical model for the prediction of the local stress and strain fields, within the representative unit cell of the unidirectional composite material. The Mixed Mode Continuum Damage Mechanics (MMCDM) theory has been utilized to model damage within the composite unit cell at the micromechanical level. The MMCDM theory enables modeling of the microdamage nonlinearities at in-plane shear and transverse compressive loadings of the composite plies. Employment of the multiscale approach enables the application of the MMCDM damage model in structural analyzes.*

*Computations at the structural level have been performed using Abaqus/Explicit, whereas the link between the two distinct scales has been established by the VUMAT subroutine. The method uses an adaptive approach in which the micromechanical computations in the HFGMC-VUMAT subroutine have been called only at the material points in which damage effects are to be expected. The Puck's ply-based failure theory has been applied as the criterion initiating the micromechanical analyzes.*

*The methodology has been implemented in the high-velocity soft-body impact simulations at T300/914 CFRP composite plates. Results of the multiscale damage model have been validated using available experimental data and by comparison with the numerical results obtained using several ply level failure criteria and the Abaqus built-in damage model for fiber-reinforced composites.*

***Keywords***: *High Fidelity Generalized Method of Cells, Multiscale analysis, Micromechanics, Abaqus/Explicit, Impact Behavior.*

*List of the most important symbols:*

$A_{ijkl}^{(\beta,\gamma)}$ - strain concentration tensor of the $\beta,\gamma$ subcell

$A^{T/C}, B^{T/C}$ - tensile/compressive post-damage slope parameters

$b_{ii}^{T/C}, b_{ij}$ - scaling parameters

$C_{ijkl}^{(\beta,\gamma)}$ - elasticity tensor of the $\beta, \gamma$ subcell

$d_i$ - secondary damage variables

$D_i^{T/C}$ - tensile/compressive scalar damage variables

$G_M^C$ - mode-specific critical strain energy release rates

$h_\beta$, $l_\gamma$ - subcell dimensions in *2* and *3* directions, respectively

$l_i$ - material length in the normal directions

$N_\beta$, $N_\gamma$ - number of subcells in *2* and *3* directions, respectively

$R_\varepsilon, Q_\varepsilon, S_\varepsilon$ - engineering shear damage initiation strains

$W_S^C$ - critical compressive strain energy

$X_{T/C}$ - fiber tensile/compressive strength

$X_\varepsilon, Y_\varepsilon, Z_\varepsilon$ - damage initiation strains in the normal directions

$\varepsilon_{ij}^{(\beta,\gamma)}$ - strain tensor of the $\beta, \gamma$ subcell

$\bar{\varepsilon}_{ij}$ - homogenized strain tensor

$\varepsilon_i^D$ - damage strains

$\bar{\sigma}_{ij}$ - homogenized stress tensor

## 1. Introduction

The complexities encountered in the damage modelling of composite structures arise from the microstructural level heterogeneities of the composite material. Consequently, multiscale approaches are becoming increasingly employed to improve the failure prediction methodologies for heterogeneous materials.

The multiscale procedure applied in this work employs Abaqus/Explicit for structural-scale high-velocity impact modelling. Micro-scale computations have been performed using the reformulated High Fidelity Generalized Method of Cells (HFGMC) to exploit the computational advantages of semi-analytical micromechanical theories which are based on the Method of Cells (MOC), after (Aboudi, 1987), (Aboudi, 2012). This particular theory has been introduced by (Bansal, 2005), (Bansal, 2006).

Results obtained in the multiscale methodology development stage have been presented in e.g. in (Ivancevic, 2014), (Smojver, 2014). This paper is focused on the structural application of the multiscale damage model. Micromechanical damage has been modelled by degradation of mechanical properties to very low values (0.01% of the undamaged values) for subcells which reach the failure state employing the relevant failure theory in e.g. (Moncada, 2008) and (Tang, 2012). In these approaches, the subsequent application of the homogenization procedure over the RUC which includes the completely degraded subcells, results in progressive degradation of the composite mechanical properties. However, the obtained progressive degradation of the homogenized properties has not been sufficient as to enable modelling of the pronounced nonlinear behavior of epoxy-based composites at in-plane shear and transverse compression loading before complete failure of the material, as discussed in (Bednarcyk, 2010). Consequently, the Mixed Mode Continuum Damage Mechanics (MMCDM) theory, introduced in (Bednarcyk, 2010), has been implemented in the micromechanical model in the described procedure to improve the accuracy of the impact damage modelling.

Validation of the methodology has been performed using available experimental data of the nonlinear behavior of the investigated T300/914 CFRP material. The numerical impact modelling procedure has been validated using the available experimental soft-body impact results in (Hou, 2007). These results have also been employed in the previous research as to validate the birdstrike damage prediction methodology in e.g. (Smojver, 2011) and (Ivancevic, 2011). The applicable experimental data is very limited in the literature and consists only of visually inspected damage states and descriptive interpretations of the final damaged states. Consequently, further validation of the multiscale methodology has been performed by comparison with the Abaqus built-in progressive damage model for fiber-reinforced composite materials.

## 2. Multiscale framework

A brief introduction to the HFGMC theory is presented in this Section to improve the completeness of the paper, whereas the complete overview of the micromechanical theory is presented in e.g. (Aboudi, 2012), (Bansal, 2006). A common aspect of the MOC-based micromechanical models is the discretization of the composite RUC into subcells which are occupied by the constituent materials. The $\beta,\gamma$ indexes are used to define the location of the individual subcells in the two dimensional RUC coordinate system $\bar{x}_2,\bar{x}_3$, which complies with the main material system of the composite ply, whereas the total number of subcells is $N_\beta \times N_\gamma$. The subcells are of rectangular shape in the implemented model, whereas all subcells are of equal size due to simplifications in the preprocessing phase, as explained in (Smojver, 2014).

The HFGMC micromechanical model has been implemented into Abaqus/Explicit using the VUMAT subroutine. The task of the micromechanical model is to determine the local strain and stress fields within the RUC, based on the applied homogenized strain state. This relation can be formulated as

$$\varepsilon_{ij}^{(\beta,\gamma)} = A_{ijkl}^{(\beta,\gamma)}\bar{\varepsilon}_{kl}\ , \quad (1)$$

where $\bar{\varepsilon}_{kl}$ is the updated homogenized strain state, which is supplied to the VUMAT subroutine based on the solution of the FE system of equations. $A_{ijkl}^{(\beta,\gamma)}$ in Equation (1) is the fourth-order strain concentration tensor which relates the local subcell strain tensor $\varepsilon_{ij}^{(\beta,\gamma)}$ to the applied homogenized strain state. The strain concentration tensors have been determined based on the solution of the HFGMC global systems of equations, employing a numerical procedure as explained in (Aboudi, 2012).

Once the micromechanical strain state has been determined, the stress field can be determined based on the constitutive equations of the individual subcells as

$$\bar{\sigma}_{ij} = \frac{1}{hl} \sum_{\gamma=1}^{N_\gamma} \sum_{\beta=1}^{N_\beta} h_\beta l_\gamma C_{ijkl}^{(\beta,\gamma)} A_{klpq}^{(\beta,\gamma)} \bar{\varepsilon}_{pq} \ , \quad (2)$$

where the *h* and *l* are dimensions of the RUC, with $h_\beta$ and $l_\gamma$ as subcell dimensions. $C_{ijkl}^{(\beta,\gamma)}$ in Equation (2) is the subcell constituent elasticity tensor, which in the applied methodology can be damaged employing the MMCDM theory, as explained in Section 3.1. The homogenized stress tensor $\bar{\sigma}_{ij}$ defines the updated stress state of the composite material which has to be calculated by the VUMAT subroutine.

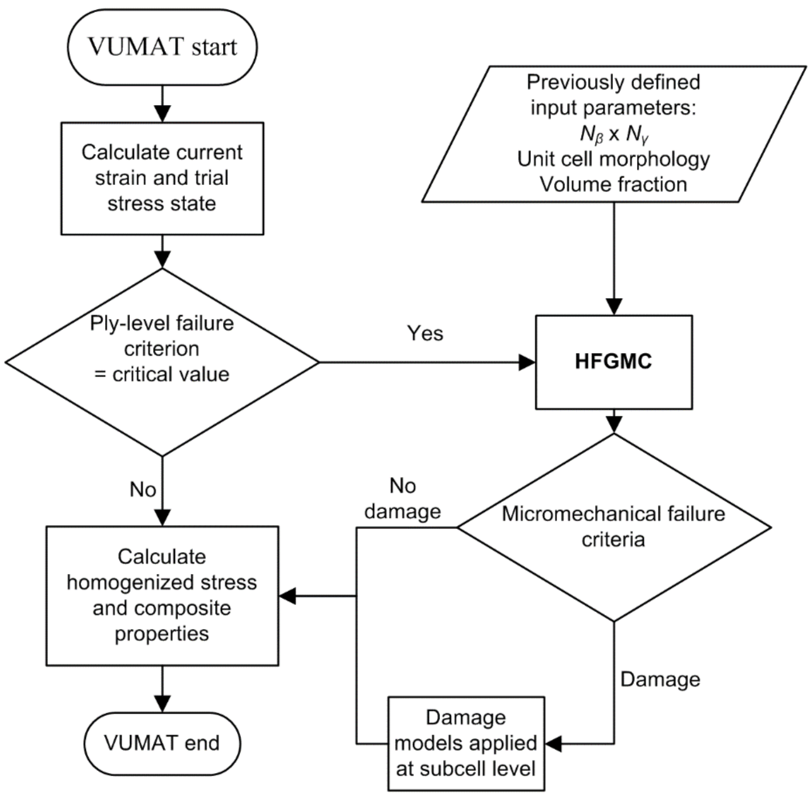


**Figure 1. Flowchart of the HFGMC VUMAT for structural damage modelling.**

Figure 1 shows the simplified VUMAT-HFGMC flowchart. The micromechanical model has been introduced into the VUMAT as a separate FORTRAN-programmed subroutine. The link between the macro-scale VUMAT and the HFGMC subroutine has been achieved using a total of 44

Solution Dependent state Variables (SDV) and 47 Common blocks. The SDVs have been employed as to visualize the maximal values of the micromechanical quantities within the RUC applied to the FE material point. For example, the maximal values of micromechanically calculated failure criteria, homogenized composite properties, and similar variables have been visualized by the SDVs in the multiscale HFGMC application.

At the start of the explicit analysis (stepTime = 0.0), the VUMAT subroutine solves a linear elastic stress update. The elasticity properties for this step have been predicted by the HFGMC subroutine before the FE analysis. The arrangement of the VUMAT subroutine utilizes an approach where the total number of material points in the FE model has been divided into blocks of variable sizes. Consequently, particular attention has to be given to the identification of each material point. This problem has been solved in the methodology by application of material point identifiers which have to be stored as COMMON variables.

Enhancement of computational aspects of the procedure has been accomplished by engaging the HFGMC computations in the VUMAT only for the material points in the structural model in which the trial stress state indicates a possibility of damage to occur. Since the impact loading is typically localized to a relatively small area, compared to the overall size of structural elements, the described adaptive multiscale approach leads to significant savings in computational time. As already described in (Smojver, 2014), where several ply-level failure initiation criteria have been compared to micromechanical damage theories, the Puck's failure theory has been employed as the criterion for the initiation of the micromechanical computations. The importance of strategies which reduce the computational cost of multiscale analyses has also been highlighted in (May, 2014) and (Otero, 2015).

## 3. Numerical model

The multiscale methodology has been applied in the high-velocity impact simulations in this paper. The numerical setup which has been employed in (Smojver, 2014), where the results of the initial stage of the methodology development have been presented, has also been used in this paper. Compared to the previous publication, the MMCDM theory has been used to simulate micromechanical damage processes at the structural scale in this work.

Soft-body impact on T300/914 plates has been analyzed in this paper. The Coupled Eulerian-Lagrangian (CEL) approach has in the numerical procedure been employed as to enable modelling of extreme deformations of the impactor. Only the most relevant features of the numerical soft-body impact modelling, which have been used in the impact analyses in this work, have been presented in this Section whereas more details are provided in (Smojver, 2014). The Abaqus built-in Mie-Grüneisen EOS has been used for the impact analyses in this work. The Mie-Grüneisen equation describes a linear relationship between the shock and particle velocities while the final form of pressure to density relation has been determined by

$$p = \frac{\rho_0 c_0^2 \eta}{\left(1 - s\eta\right)^2}\left(1 - \frac{\Gamma_0 \eta}{2}\right) + \Gamma_0 \rho_0 U_m, \quad (3)$$

where $\eta = 1 - \rho_0 / \rho$ is the nominal volumetric compressive strain, $\rho_0$ is the initial density, $\Gamma_0$ is a material constant and $U_m$ is the internal energy per unit mass, as defined in the Abaqus Users

Manual. The employed EOS parameters have been validated in (Smojver, 2012), and take the values $\rho_0 = 1010\ \mathrm{kg/m^3}$, $c_0$ = 1480 m/s (speed of sound in the material), $\Gamma_0 = 0$ and $s$ = 0 (coefficient defining the linear relationship between shock and particle velocities).

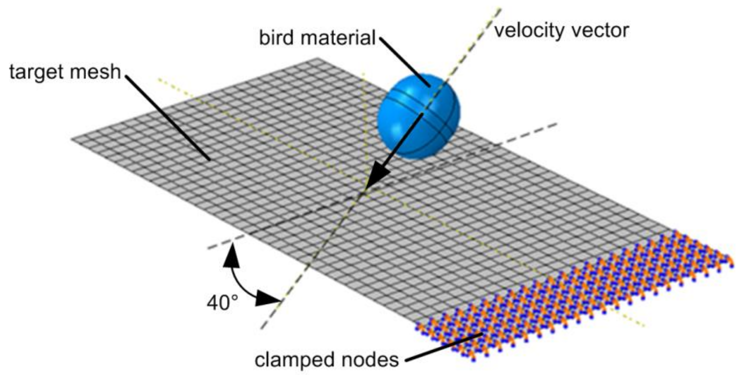


**Figure 2. Setup of the numerical multiscale model.**

The numerical model, with the applied initial and boundary conditions, is shown in Figure 2. The simulated impact cases replicate two impact cases for which results of the gas gun experiment have been provided in (Hou, 2007). The velocity vector of the impacting material is inclined at 40° with regard to the target plate, whereas the clamped nodes at one of the ends of the plate simulate the clamps used in the experiments. A magnitude of 200 m/s has been applied to the Eulerian material of the impactor in the first impact case, whereas this value has been increased to 280 m/s in the second analyzed case.

The diameter of the gelatine projectile is 25 mm with the mass of 10 g. The shape of the substitute bird has been modelled as a cylinder with hemispherical ends. Dimensions of the CFRP plate are 216 x 102 mm. The total thickness of the plate is 3 mm, with the $[(0/90)_5/\overline{0}\,]_S$ layup.

The size of the cube containing 487,920 Eulerian elements is 0.45 x 0.4 x 0.2 m, as the Eulerian material should not leave this volume to promote numerical stability of the analysis, as described in (Smojver, 2011).

## 3.1 Micromechanical damage model

Conclusions drawn from the initial applications of failure models in MOC-based micromechanical models are that progressive damage mechanics principles need also to be included in the micromechanical theories, as highlighted in Section 1. Due to the limitations of this manuscript, only the final relations have been provided here.

The theory relies on the damage strains, defined as

$$\varepsilon_1^D = \sqrt{\left(\frac{\varepsilon_{11}}{X_\varepsilon}\right)^2 + \left(\frac{\gamma_{13}}{R_\varepsilon}\right)^2 + \left(\frac{\gamma_{12}}{S_\varepsilon}\right)^2}, \quad (4)$$

$$\varepsilon_2^D = \sqrt{\left(\frac{\varepsilon_{22}}{Y_\varepsilon}\right)^2 + \left(\frac{\gamma_{23}}{Q_\varepsilon}\right)^2 + \left(\frac{\gamma_{12}}{S_\varepsilon}\right)^2}, \quad (5)$$

$$\varepsilon_3^D = \sqrt{\left(\frac{\varepsilon_{33}}{Z_\varepsilon}\right)^2 + \left(\frac{\gamma_{23}}{Q_\varepsilon}\right)^2 + \left(\frac{\gamma_{13}}{R_\varepsilon}\right)^2}, \quad (6)$$

to predict microdamage initiation of the matrix subcells. The varaibles $X_\varepsilon$, $Y_\varepsilon$, $Z_\varepsilon$ in Equations 4-6 are damage initiation strains in the principal material axes directions whereas $R_\varepsilon$, $Q_\varepsilon$ and $S_\varepsilon$ are engineering shear damage initiation strains. Failure initiation in the fiber subcells is modelled as the maximum stress in the fiber direction criterion

$$\left(\frac{\sigma_{11}^{(\beta,\gamma)}}{X_{T/C}}\right)^2 \geq 1. \quad (7)$$

Continuum Damage Mechanics principles have been introduced to degrade the elasticity properties of matrix subcells in the MMCDM model, whereas fiber subcell properties are completely degraded if the criterion defined in Equation 7 is satisfied. The progressive damage effects in the matrix subcells have been enforced by employing six scalar damage variables which are tensile and compressive damage variables in each of the three principal material orientations, $D_i^{T/C}$. The matrix subcell elasticity properties have been degraded employing

$$E_i = d_i E^0, \quad i = 1,2,3, \quad (8)$$

and

$$\nu_{ij} = d_i \nu^0, \quad i, j = 1,2,3. \quad (9)$$

The secondary damage variables in Equations 8 and 9 are defined as

$$d_i = 1 - b_{ii}^{T/C} D_i^{T/C}, \quad i = 1,2,3, \quad (10)$$

where $b_{ii}^{T/C}$ are scaling parameters, which take different values in tensile and compressive loading. The shear stiffness components have been degraded employing the appropriate damage variables as

$$\begin{aligned} G_{23} &= \left(1 - b_{42} D_2^{T/C} - b_{43} D_3^{T/C}\right) G^0, \\ G_{13} &= \left(1 - b_{51} D_1^{T/C} - b_{53} D_3^{T/C}\right) G^0, \quad (11) \\ G_{12} &= \left(1 - b_{61} D_1^{T/C} - b_{62} D_2^{T/C}\right) G^0, \end{aligned}$$

where $b_{ij}$ are scaling parameters while $G^0$ is the undamaged shear modulus of the matrix. Evolution of the six damage variables has been derived by considering the stress-strain curves for uniaxial loading of the constituents in (Bednarcyk, 2010). The incremental change of the damage variables $dD_i$ is

$$dD_i = \left(1 - D_i - A\exp\left(-\varepsilon_i^D / B\right)\right)\frac{d\varepsilon_i^D}{\varepsilon_i^D}, \quad i = 1,2,3, \qquad (12)$$

where $A$ and $B$ are the post-damage slope parameters, which define the constitutive behavior of the damaged matrix material, and $d\varepsilon_i^D$ is the current increase of the damage strains. Subcell failure has been modelled in the MMCDM theory by application of damage energy principles. The approach employs different formulations for subcell failure in tensile and compressive loading modes. Consequently, a mode-specific strain energy release rate criterion has been used for the tensile loading modes, whereas failure in compressive load cases has been predicted using the total released energy. More details of the described approaches are provided in (Bednarcyk, 2010). Subcell failure has been modelled by applying very low values (0.01%) to the secondary damage variables in Equations 8 and 9.

## 3.2 Validation of the micromechanical damage model

The validation of the implementation of the MMCDM model into the HFGMC model and the multiscale procedure has been accomplished using the standalone HFGMC application, as described in (Ivancevic, 2014). An important part during this process has been the investigation of the damage effects within the composite RUC for various load cases. The evaluation of the MMCDM theory results within the RUC has been performed as to assess the micromechanical effects of the progressive degradation model on the homogenized composite behavior. Analyses of the local parameters of the damage model at various homogenized load cases provide the link between the local fields and the composite's response. Conclusions drawn from these analyses have been essential for the interpretation of the MMCDM multiscale application since the SDVs, employed to visualize results of the micromechanical analysis in the multiscale framework, show only the maximal values of an individual parameter within the RUC, as explained in Section 2.

**Table 1. T300/914 constituent properties.**

| | | | | |
|---|---|---|---|---|
| **T300 fibre** | | | | |
| $E_1$ [GPa] | $E_2 = E_3$ [GPa] | $G_{12} = G_{13}$ [GPa] | $G_{23}$ [GPa] | $\nu_{23}$ [-] |
| 230.0 | 18.5 | 19.0 | 12.0 | 0.4 |
| $\nu_{12} = \nu_{13}$ [-] | $X_T$ [GPa] | $X_C$ [GPa] | | |
| 0.2 | 2.5 | 1.5 | | |
| **914 matrix** | | | | |
| $E$ [GPa] | $\nu$ [-] | $X_\varepsilon^T, Y_\varepsilon^T, Z_\varepsilon^T$ [-] | $X_\varepsilon^C, Y_\varepsilon^C, Z_\varepsilon^C$ [-] | $R_\varepsilon, Q_\varepsilon, S_\varepsilon$ [-] |
| 4.6 | 0.35 | 0.0059 | 0.032 | 0.034 |

An important conclusion obtained from the RUC analyses is that the composite material becomes unable to resist any significant loads in the matrix dominated loadings at the state at which 15% of matrix subcells have failed. This condition corresponds to the change of damaging mode from matrix microdamage to transverse matrix cracking and has therefore been employed as the material point failure criterion in the multiscale analyses.

**Table 2. 914 matrix MMCMD parameters.**

| $G_I^C\left[\mathrm{J/m^2}\right]$ | $G_{II}^C = G_{III}^C\left[\mathrm{J/m^2}\right]$ | $W_S^C\,[\mathrm{J}]$ | $l_i\,[\mathrm{m}]$ | $A^T\,[-]$ | $B^T\,[-]$ | $A^C = B^C\,[-]$ | $b_{ii}^T = b_{ii}^C\,[-]$ | $b_{4i} = b_{5i} = b_{6i}\,[-]$ |
|---|---|---|---|---|---|---|---|---|
| 800. | 2400. | $1.86\times10^{-6}$ | $9.\times10^{-6}$ | 0.70 | 1.10 | 1.00 | 1.32 | 0.50 |

The constituent elasticity properties and the damage initiation strains for the 914 matrix are provided in Table 1. Orthotropic mechanical properties have been employed for the T300 carbon fiber while an isotropic constitutive model has been applied for the matrix subcells. An increased matrix elasticity modulus, compared to the value provided in (Soden, 1998), has been applied in the analysis as to match the defined composite properties.

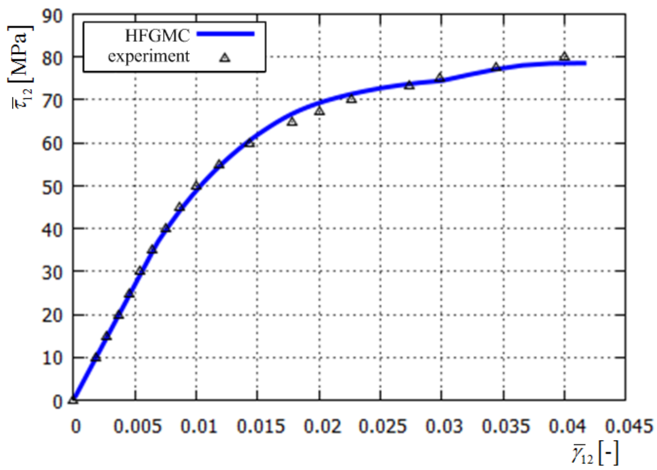


**Figure 3. In-plane shear response of the T300/914 material.**

The MMCDM damage model parameters for the 914 matrix, which have been employed throughout this work, are provided in Table 2. The post-damage slope parameters of the MMCDM model for the T300/914 composite have been determined by considering the nonlinear response of the material in the in-plane shear loading condition, after (Soden, 1998). Parameters of the MMCDM model final subcell failure criterion have been assumed equal to the values provided in (Bednarcyk, 2010) for the MY750 matrix. This assumption has been justified by the fact that both matrices are epoxy polymers of the similar mechanical behavior.

Figure 3 shows the response of the homogenized material, compared against the experimental results, in the in-plane shear loading conditions. The micromechanical computations have been performed using a 30x30 RUC with the single fiber inclusion in the center.

## 4. Multiscale Results

Results of the ply-level failure analyzes using the Abaqus progressive damage model for unidirectional composites, provided in (Smojver, 2011), indicate that simulation of 0.4 ms is necessary for the prediction of the final state of damage at the impact location at the 200 m/s impact. The T300/914 elasticity components and ply strengths have been taken from (Lachaud, 1997). The damage initiation strains, employed in the multiscale analyses, have been modified as to account for the higher ply strength properties of the T300/914 composite provided in (Lachaud, 1997) compared to the values provided in (Soden, 1998). The employed damage initiation strains are provided in Table 3, while the MMCDM damage parameters, which are presented in Table 2, have not been modified in the multiscale analyses.

**Table 3. 914 matrix damage initiations strains in the multiscale analyzes.**

| $X_\varepsilon^T, Y_\varepsilon^T, Z_\varepsilon^T$ [-] | $X_\varepsilon^C, Y_\varepsilon^C, Z_\varepsilon^C$ [-] | $R_\varepsilon, Q_\varepsilon, S_\varepsilon$ [-] |
|---|---|---|
| 0.012 | 0.036 | 0.041 |

Accuracy of the micromechanical computations has been ensured by application of a time increment of $1.5\times10^{-8}$ s in the 200 m/s impact analysis as to keep the strain increment, which is applied to the HFGMC micromodel, to an acceptable level. The value of the strain increment, at which the applied HFGMC solution scheme provides accurate results, has been determined using the standalone application by comparison of the micromechanical results with the experimentally obtained composite failure curves and nonlinear behavior at the in-plane shear and compressive loading conditions of the composite material.

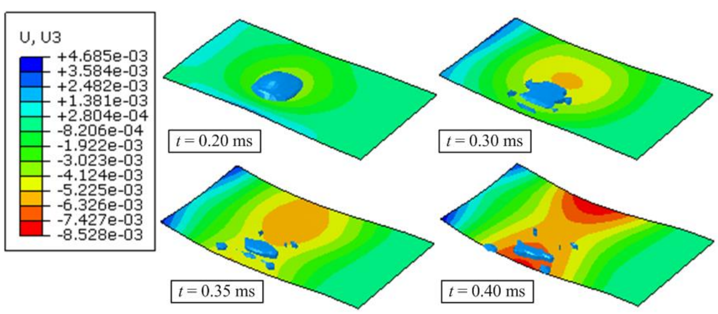


**Figure 4. 200 m/s impact event on T300/914 plate, contours show displacements in *z* direction, [m].**

The impact event with contours of the plate displacements in the *z* direction is shown in Figure 4. The results presented in Figure 4 have been computed using the multiscale methodology, whereas the referent Abaqus damage model simulation indicates similar peak values of the displacements.

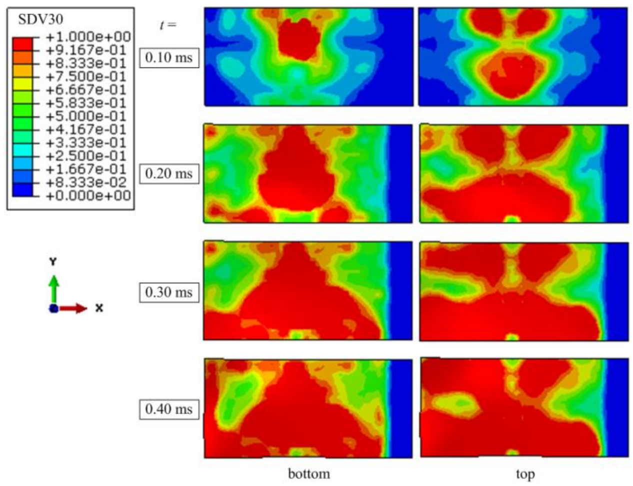


**Figure 5. Evolution of the $\varepsilon_2^D$ damage strain at the 200 m/s impact on the T300/914 composite plate.**

As explained in Section 2, the SDVs associated with micromechanical failure criteria and damage variables show the maximal values within the RUC associated with the relevant FE material point. The predominant mode of failure in the analyzed impact case is matrix damage initiated by the high values of the $\varepsilon_2^D$ damage strain. The damage strains, as micromechanical failure initiation criteria in the MMCDM theory, indicate damage initiation at the subcell level at the material points located at the impacted side of the plate (referred to as "top ply" throughout this work) as well as in the material points located at the opposite side of the impact (referred to as "bottom ply"). As defined by the layup of the plate, both of these plies are aligned with the longer plate dimension (0° plies). Visualization of the evolution of the $\varepsilon_2^D$ damage strain for the top and bottom composite plies is shown in Figure 5.

The final state of damage, as predicted by the multiscale analysis is shown by the contours of fractions of failed subcells in Figure 6. The material points for which the results in this Figure are shown belong to the bottom ply in which the damage effects are more pronounced due to the lower damage initiation strains in tensile loading modes compared to the relevant compressive values. These results are supported by the results of the Abaqus damage model which are presented in Figure 6 by the matrix tensile damage parameter DAMAGEMT. These contours agree relatively well to the fractions of failed subcells predicted by the MMCDM model.

The fiber failure micromechanical criterion indicates damage onset in several 0° plies at the clamped plate end. This damage mode has been caused by the structural (flexural) response of the plate. This failure mode is shown in Figure 6 by the failed subcells near the clamped edge of the plate which is located at the right-hand side in the presented images.

Schematic representation of the visually observed impact damage is shown in Figure 6 (image at the top), after (Hou, 2007). Although C-scan images have been provided in (Hou, 2007) for some impact cases (mostly for woven composites), only visual observation of the impact damage has been provided for the T300/914 impacts. The C-scans would be very useful for the validation of the numerical damage prediction methodology, using the locations and sizes of the detected matrix cracks and delaminations as references for validation and calibration of the multiscale damage model.

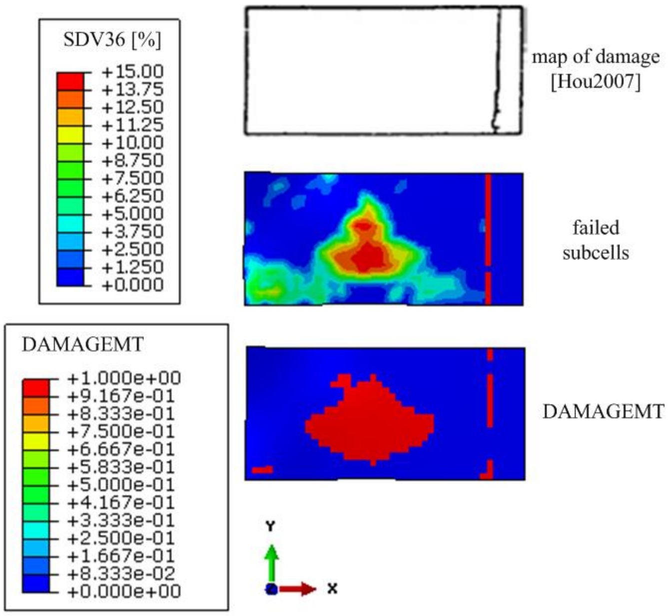


**Figure 6: Comparison of the numerical results with the experimental results provided in (Hou, 2007) for the 200 m/s impact.**

Simulation of the 280 m/s impact has been performed employing a time step of $1\times10^{-8}$ s for the multiscale explicit analysis. The extreme loading conditions initiate damage processes in a very large part of the composite plate throughout the analysis, causing long computational times. Consequently, only 0.275 ms of the impact event has been analyzed employing the multiscale approach as to keep the computational time at an acceptable level.

The experimental study of the 280 m/s impact resulted in complete perforation of the composite plate with fiber failure, matrix cracking and delamination damage modes, after (Hou, 2007). The visually observed damage pattern is shown in Figure 7. This Figure shows also the contours of fractions of failed subcells predicted by the multiscale analysis. Only two finite elements have been removed from the model in the multiscale analysis, indicating that the numerical result does not predict complete perforation of the plate in this analysis. However, contours of the fractions of the failed matrix subcells (as shown in Figure 7 for the bottom composite ply) resemble the visually observed damage state from the gas gun experiment. In contrast to the 200 m/s impact case, the multiscale analysis, as well as the Abaqus damage model, predict fiber failure in the composite plate at the impact location.

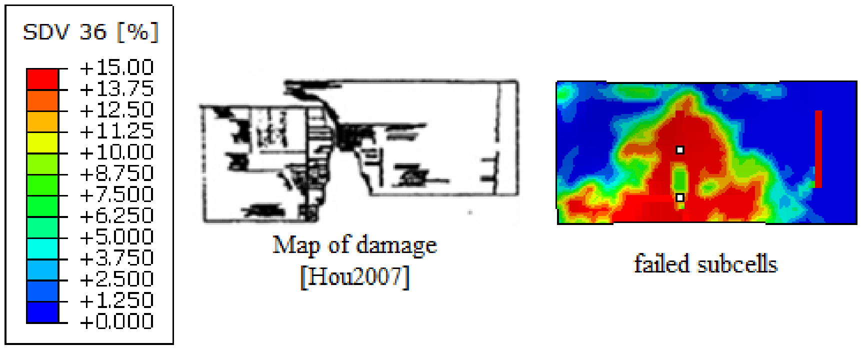


**Figure 7: Comparison of multiscale analysis and experimentally observed damage state.**

The Abaqus damage model also predicts very large extent of damage in the plate. However, only one element has reached the criterion for element failure in the analysis. Visualization of the impact event is shown in Figure 8. The contours in this image visualize the matrix tensile damage variable. Despite the extensive damage predicted by the model, only one finite element has been removed from the analysis, causing nonphysical response of the plate at later time steps, which could be attributed to plate perforation. This conclusion indicates that a total time of approximately 0.6 ms should be analyzed as to predict the plate perforation. However, this analysis would be computationally too expensive considering the available computational resources.

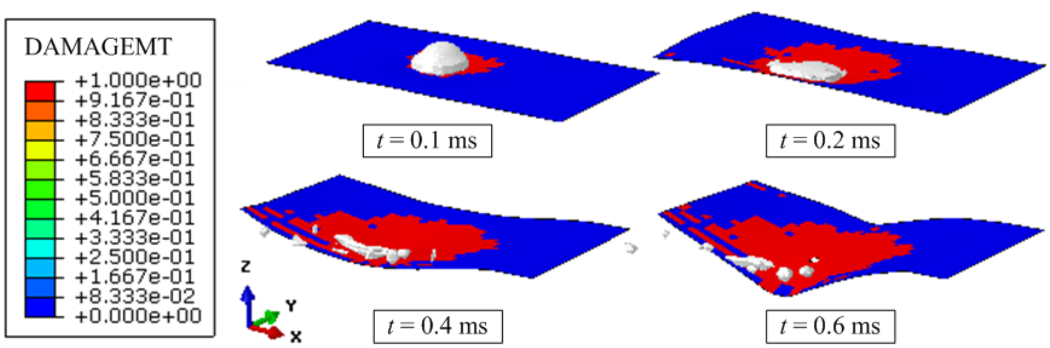


**Figure 8. Visualization of the impact event at 280 m/s, predicted by the Abaqus damage model.**

## 5. Conclusions

Although the FE model applied in the impact analyses is relatively small, application of the multiscale approach transforms the numerical model into a computationally very demanding task.

The conclusions obtained from the performed analyses highlight the importance of computationally efficient, as well as accurate, micromechanical models.

Complete compliance with experimental results is difficult to obtain as numerical prediction of a complex phenomena, e.g. perforation of composite plates, is a highly difficult task. The numerical results indicate that the damage parameters reach maximal values in the location where the plate broke into two halves in the experiment. Consequently, it can be concluded that the physical phenomenon has been modelled with acceptable accuracy. Excellent agreement between the multiscale analyses employing the MMCDM theory and the Abaqus built-in progressive damage model has also been achieved in the analyses, providing confidence in the further development of the methodology.

## 6. References


1. Abaqus Users Manual, Version 6.10-1, Dassault Systémes Simulia Corp., Providence, RI.
2. Aboudi, J., "Closed Form Constitutive Equations for Metal Matrix Composites," International Journal of Engineering Science, vol. 25, no. 9, pp. 1229-1240, 1987.
3. Aboudi, J., Arnold, S.M., and B.A. Bednarcyk, "Micromechanics of Composite Materials – a Generalized Multiscale Analysis Approach," Elsevier Science Ltd., 2012.
4. Bansal, Y., and M.-J. Pindera, "A Second Look at the Higher-Order Theory for Periodic Multiphase Materials," Journal of Applied Mechanics, vol. 72, no. 2, pp. 177-195, 2005.
5. Bansal, Y., and M.-J. Pindera, "Finite-Volume Direct Averaging Micromechanics of Heterogeneous Materials with Elastic-Plastic Phases," International Journal of Plasticity, vol. 22, no. 5, pp. 775-825, 2006.
6. Bednarcyk, B.A., Aboudi, J., and S.M. Arnold, "Micromechanics Modeling of Composites Subjected to Multiaxial Progressive Damage in the Constituents," AIAA Journal, vol. 48, no. 7, pp. 1367-1378, 2010.
7. Hou, J.P., and C. Ruiz, "Soft Body Impact on Laminated Composite Materials," Composites Part A: Applied Science and Manufacturing, vol. 38, no. 2, pp. 505-515, 2007.
8. Ivančević, D., and I. Smojver, "Hybrid Approach in Bird Strike Damage Prediction on Aeronautical composite structures," Composite Structures, vol. 94, no.1, pp. 15-23, 2011.
9. Ivančević, D., and I. Smojver, "Micromechanical Damage Modelling Using a Two-Scale Method For Laminated Composite Structures," Composite Structures, vol. 108, pp. 223-233, 2014.
10. Lachaud F., Lorrain B., Michel L., and R. Barriol, "Experimental and numerical study of delamination caused by local buckling of thermoplastic and thermoset composites," Composites Science and Technology, vol. 58, no. 5, pp. 727-733, 1997.
11. May, M., Nossek, M., Petrinic, N., Hiermaier, S., and K. Thoma, "Adaptive multi-scale modeling of high velocity impact on composite panels," Composites Part A: Applied Science and Manufacturing, vol. 58, pp. 56-64, 2014.
12. Moncada, A.M., Chattopadhyay, A., Bednarcyk, B.A., and S.M. Arnold, "Micromechanics-based progressive failure analysis of composite laminates using different constituent failure theories," Journal of Reinforced Plastics and Composites, vol. 31, no. 21, pp. 1467-1487, 2008.

13. Otero, F., Martines, X., Oller, S., and O. Salomon, “An efficient multi-scale method for non-linear analysis of composite structures,” Composite Structures, vol. 131, pp. 707-719, 2015.
14. Smojver, I., and D. Ivančević, “Bird Strike Damage Analysis in Aircraft Structures Using Abaqus/Explicit and Coupled Eulerian Lagrangian Approach,” Composites Science and Technology, vol. 71, no. 4, pp. 489-498, 2011.
15. Smojver, I., and D. Ivančević, “Advanced Modelling of Bird Strike on High Lift Devices Using Hybrid Eulerian–Lagrangian Formulation,” Aerospace Science and Technology, vol. 23, no. 1, pp. 224-232, 2012.
16. Smojver, I., and Ivančević, D.,” Multiscale Modeling of High Velocity Impact Damage on Composite Structures,” 2014 SIMULIA Community Conference.
17. Soden, P.D., Hinton, M.J., and A.S. Kaddour, “Lamina Properties, Lay-up Configurations and Loading Conditions for a Range of Fibre-Reinforced Composite Laminates,” Composites Science and Technology, vol. 58, no. 7, pp. 1011-1022, 1998.
18. Tang Z., and B. Zhang, “Prediction of biaxial failure envelopes for composite laminates based on Generalized Method of Cells,” Composites Part B: Engineering, vol. 43, no. 3, pp. 914-925, 2012.